

Cooperative Effect of Adsorbed Cations and Iodide on the Interception of Back Electron Transfer in the Dye Sensitization of Nanocrystalline TiO₂

Serge Pelet, Jacques-E. Moser,* and Michael Grätzel

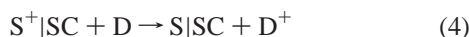
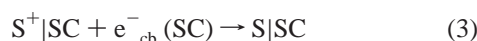
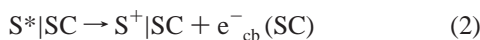
Laboratory for Photonics and Interfaces, Institute of Physical Chemistry,
Ecole Polytechnique Fédérale de Lausanne, 1015 Lausanne, Switzerland

Received: September 27, 1999; In Final Form: December 9, 1999

Specific adsorption of cations (H⁺, Li⁺, ...) on TiO₂ nanocrystalline particles is known to control the energetics of the conduction band and therefore the ability for molecular sensitizers to inject electrons into the semiconductor upon irradiation. In photoelectrochemical energy conversion devices employing dye-sensitized titanium dioxide mesoporous electrodes, back electron transfer is generally intercepted by the use of the iodide/triiodide couple as a charge mediator. Kinetics of the oxidation of I⁻ by the oxidized state of *cis*-Ru^{II}-(dcbpy)₂(NCS)₂ sensitizer adsorbed on TiO₂ was measured by flash photolysis in propylene carbonate. The rate of this reaction was found to depend on the nature and concentration of added cations such as Mg²⁺, Li⁺, Na⁺, and K⁺. A brusque acceleration of the process was in particular observed at a critical concentration. Electrophoretic measurements showed that this step in the dye regeneration reaction kinetics corresponds to the reversal of particle surface charge upon adsorption of potential-determining species, which causes I⁻ to efficiently adsorb onto the oxide. These observations strongly suggest that the specific adsorption of cations on TiO₂ nanoparticles governs the formation of (I⁻, I⁻) ion pairs on the surface, and allows the more energetically favorable and faster mechanism involving oxidation of I⁻ to I₂^{•-} radical to take place.

Introduction

Upon irradiation, redox dye photosensitizers (S) adsorbed on the surface of wide band gap metal oxide semiconductors readily inject an electron in the conduction band of the solid. Charge injection (eq 2) has been found for numerous efficient systems to be a very fast process that occurs in the femtosecond time frame.^{1,2} In the absence of electrolyte, the electron back transfer (eq 3) takes place more slowly, typically in the microsecond–millisecond time domain.^{3,4} This charge recombination process can be intercepted by reaction of a reducing mediator with the oxidized dye (eq 4). The overall efficiency of the light-induced charge separation then depends on the kinetic competition between back electron transfer and dye regeneration processes.⁴



Photovoltaic cells based on the sensitization of titanium dioxide by Ru(II) complex dyes and using the I⁻/I₃⁻ redox couple as a mediator have proved very efficient at exploiting this principle.^{4,5} In such systems, the ionic mediator travels back and forth by diffusion from working to counter electrodes to shuttle to the sensitizer the electrons that have gone through the electrical circuit. The rate of the reaction between the Ru(III)-centered oxidized dye and iodide following charge injection is crucial for the efficiency of the energy conversion device. The faster the rate of reaction 5, the more electrons are forced to leave the semiconductor and contribute to the photocurrent.



Surprisingly, very little is understood about the actual processes that lead to the dye regeneration. In particular, the mechanism of the two-electron transfer reaction (eq 5) has not been clearly established and many factors appear to influence its rate.^{6,7}

The following one-electron transfer reactions can in principle take place on the surface of the oxide and account globally for the oxidation of iodide to triiodide:⁷



Oxidation of iodide to I₂^{•-} radical is obviously more thermodynamically favorable than the reaction leading to iodine atom.⁸ Assuming a normal kinetic behavior, reaction 8 is expected to offer a faster pathway, provided that (I⁻, I⁻) or (S⁺, I⁻) ion pairs are present in significant amount.⁷ Providing the surface carries a sufficient positive charge, iodide could electrostatically adsorb onto the surface and form (I⁻, I⁻) pairs in the vicinity of the oxidized sensitizer.

Recent works have shown that adsorption on the oxide surface of potential-determining cations has a strong effect on the injection rate and quantum yield.⁹ Similarly, specific adsorption of cations on TiO₂ particles is expected to electrostatically control the association of I⁻ with the oxide surface and/or with the adsorbed dye molecules and consequently govern the rate of the regeneration reaction 5.

We report here on the kinetics of the oxidation of iodide in the sensitization of nanocrystalline TiO₂ films by Ru^{II}(dcbpy)₂-

* Corresponding author. E-mail: je.moser@epfl.ch.

(NCS)₂ complex dye. The effect of the nature and concentration of counterions on the rate of the dye regeneration is more particularly addressed. In addition to laser flash photolysis experiments, electrophoretic measurements have allowed for a qualitative understanding of the role played by specifically adsorbed cations, which are able in defined conditions to reverse the sign of the charge (ζ -potential) of sensitized titanium dioxide particles from negative to positive.

Methods

Transient Laser Spectroscopy. Transparent mesoporous TiO₂ layers (thickness 7–10 μm) were prepared on a glass substrate using a previously reported procedure.^{5b,10} Dry nanocrystalline titania films were dyed by adsorption of the sensitizer, [*cis*-Ru^{II}(2,2'-bipyridyl-4,4'-dicarboxylate-H)₂(NCS)₂]²⁻ (TBA⁺)₂, from an ethanolic solution. A drop of pure solvent or of the electrolyte was then sandwiched between the sample and a thin microscope coverglass. Anhydrous propylene carbonate (Fluka, <50 ppm of H₂O) was used as the solvent throughout all experiments described hereafter.

Samples were subjected to flash photolysis immediately after preparation, although they appeared to be remarkably stable. Pulsed laser excitation was applied using a GWU-350 broadband optical parametric oscillator pumped by a Continuum Powerlite-7030 frequency-tripled Q-switched Nd:YAG laser ($\lambda = 355$ nm, 30 Hz repetition rate). The output of the OPO (pulse width at half-height ≈ 5 ns) was tuned at $\lambda = 490$ nm and attenuated to ≤ 1 mJ/pulse. The beam was expanded by a planoconcave lens to irradiate a large cross section (≥ 1 cm²) of the sample, whose surface was kept at a 45° angle to the excitation and probe beams. The analyzer light, produced by a CW 450 W Xe arc lamp, was passed through a first monochromator, various optical elements, the sample, and a second monochromator, prior to being detected by a fast PM tube. A 1 GHz band-pass digital signal analyzer was employed to record the time course of the optical absorbance changes induced by laser excitation of the films. Satisfactory signal-to-noise ratios were typically obtained by averaging over 10–100 laser shots.

Electrophoresis. Electrophoretic measurements were realized with a Rank Bros. Mark II instrument, equipped with a quartz capillary cell of circular cross section. An ultramicroscope assembly, consisting of a He–Ne laser for dark-field illumination, a microscope objective, and a CCD camera, allowed the observation of the particles movement upon application of an electric field to the ends of the capillary. TiO₂ powder (Degussa, P25) was heated at 450 °C in air to remove adsorbed water and most of surface hydroxyl groups. The treated titania was then dispersed in dry propylene carbonate to yield a transparent stable colloid of ca. 0.2 g/L. Electrokinetic ζ -potentials of the particles were calculated from the value of the applied electric field E and the measured particle velocity v using the Henry equation,¹²

$$\zeta = \frac{3v\eta}{2\epsilon E f(\kappa a)} \quad (10)$$

where η is the solvent viscosity, ϵ its static dielectric constant, and $f(\kappa a)$ a function, which varies smoothly from 1 to 1.5, depending on the particle radius (a) and the ionic strength of the electrolyte.¹²

Results and Discussion

Figure 1A shows the time evolution of the transient absorption spectra observed with *cis*-Ru^{II}(dcbpy)₂(NCS)₂-sensitized TiO₂ in pure propylene carbonate. A broad negative feature is

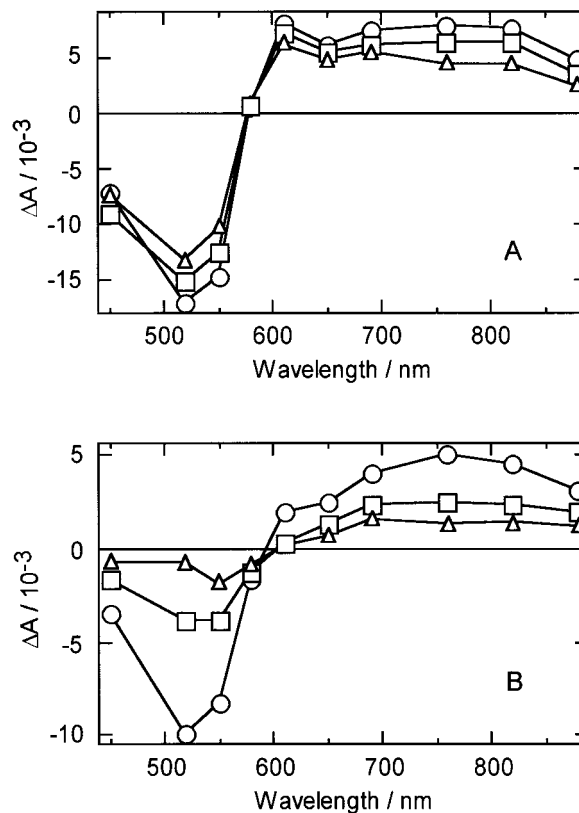


Figure 1. Transient absorption spectra obtained upon nanosecond pulsed laser excitation of Ru(II)(dcbpy)₂(NCS)₂ dye adsorbed on nanocrystalline TiO₂ in dry propylene carbonate, without electrolyte (A), and in the presence of tetrabutylammonium iodide TBAI 0.5 M (B). Absorbance changes are recorded 50 (—○—), 200 (—□—), and 800 ns (—△—) after the laser excitation ($\lambda = 490$ nm, 5 ns pulse duration) was applied.

observed between 450 and 580 nm, which is assigned to the bleaching of the dye ground-state absorption upon electronic excitation and electron injection into the titanium dioxide. A positive feature is observed above 580 nm that is due to the absorption of the oxidized sensitizer (S⁺) produced by the subpicosecond charge injection process.^{1c,11} The injection quantum yield was found under these conditions to be practically unity.² In the absence of any other redox-active species, the only mechanism for dye regeneration is back electron transfer from the conduction band of the solid to the oxidized sensitizer (eq 3). This recombination process is relatively slow, as only a minor portion of the ground-state absorption of the dye is recovered in the submicrosecond time scale.

The result of a similar experiment carried out in the presence of TBAI 0.5 M is displayed in Figure 1B. In this case, regeneration of the original dye absorption following charge injection is clearly faster, indicating that I⁻ was able to efficiently intercept the oxidized sensitizer.

Figure 2 represents the transient absorption kinetics recorded in propylene carbonate with various electrolytes added. In all cases, the recovery of the ground-state absorption of the dye, after the fast electron injection into the solid, does not follow a simple kinetic law.^{3c} In the absence of any electrolyte (trace a), the time needed to reach half of the initial absorbance ($t_{1/2}$) through back electron transfer is 2 μs . Total recovery of the initial absorption, though, requires several hundreds of microseconds. Traces b, c, and d were recorded after addition of a common concentration of 0.1 M of iodide in the form of tetrabutylammonium (TBA⁺), Li⁺, and Mg²⁺ salts, respectively. While addition of the electrolyte in all three cases leads to an

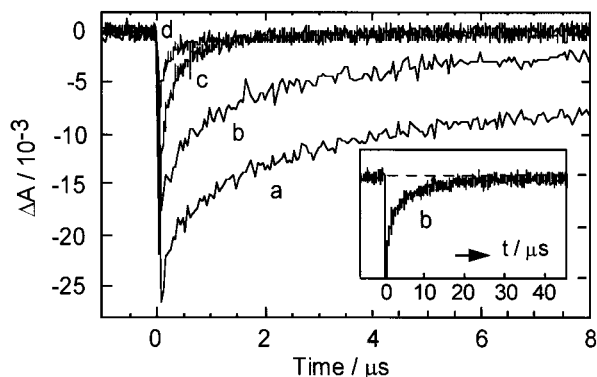


Figure 2. Time course of the transient absorbance changes obtained upon nanosecond pulsed laser excitation ($\lambda = 490$ nm, 5 ns fwhm pulse duration, 1 mJ/pulse) of Ru(II)(dcbpy)₂(NCS)₂ dye adsorbed on mesoporous TiO₂ films. Bleaching signals were measured at $\lambda = 520$ nm in dry propylene carbonate, without electrolyte (a), and in the presence of TBAI 0.1 M (b), LiI 0.1 M (c), and MgI₂ 0.05 M (d). The insert displays trace (b) on a longer time scale.

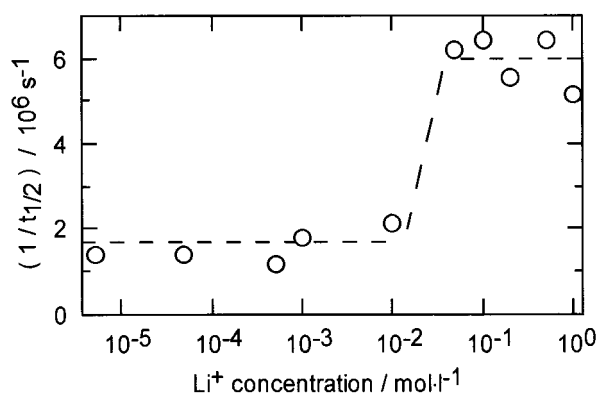


Figure 3. Reciprocal half-lifetime ($1/t_{1/2}$) of the Ru(II)(dcbpy)₂(NCS)₂ dye ground-state absorbance recovery ($\lambda = 520$ nm) following electron injection into TiO₂. Concentration of iodide [I^-] = 0.1 M in anhydrous propylene carbonate was kept constant, while the concentration of Li⁺ cations was varied. Up to 0.1 M Li⁺, iodide counterions are TBA⁺ and Li⁺. At higher concentrations, Li⁺ was added in the form of dry LiClO₄.

acceleration of the dye regeneration, the kinetics of the S⁺ state reduction by I⁻ appears to depend strongly upon the nature of the cation used. With Li⁺ and Mg²⁺, the total recovery of the dye is completed in less than 4 μ s, while about 40 μ s are necessary for TBA⁺.

The influence of the concentration of the potential-determining cation Li⁺ on the kinetics of reaction 5 was studied in the presence of a fixed concentration of I⁻. Results of laser kinetic measurements reported in Figure 3 show that, for low concentrations of lithium ions added ($\leq 10^{-2}$ M), the reciprocal half-lifetime of the dye regeneration process $1/t_{1/2} = 1.7 \times 10^6$ s⁻¹ remains constant and is similar to the value obtained with 0.1 M TBAI and no Li⁺. Between 10^{-2} M and 5×10^{-2} M Li⁺, the measured value of $1/t_{1/2}$ rises abruptly to stay approximately constant as the concentration is further increased. A similar behavior was observed for the addition of Mg²⁺ ions. In this case, however, the step in the reaction kinetics appears even at a lower concentration (10^{-3} – 10^{-2} M).

Although LiClO₄ and Mg(ClO₄)₂ salts used in the experiments were carefully dried by heating under vacuum, addition of these highly hygroscopic compounds inevitably introduce some water in the initially anhydrous solvent. The amount of H₂O contained in the electrolyte was thus measured using Karl Fischer coulometric titration and was found to be in all cases lower

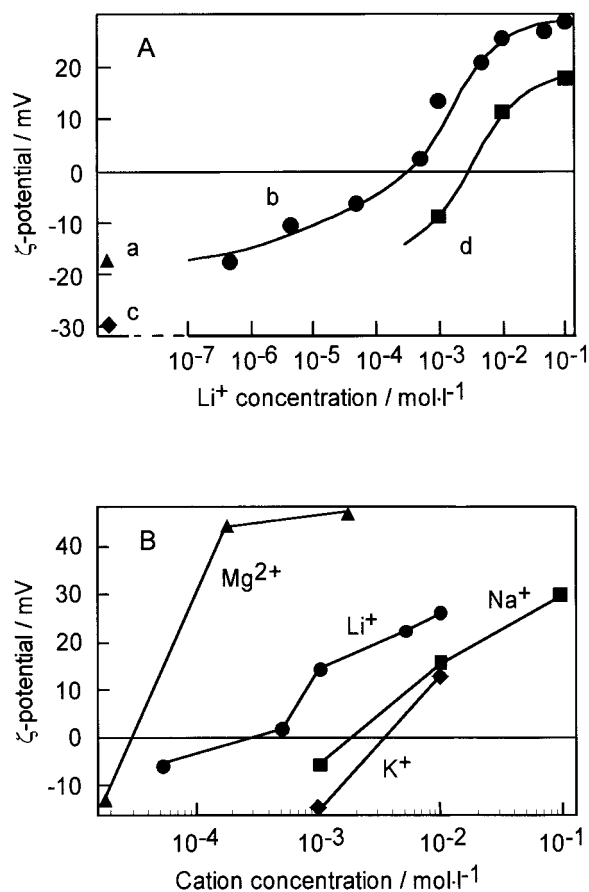


Figure 4. ζ -potential of TiO₂ nanoparticles dispersed in dry propylene carbonate determined by electrophoresis as a function of added cations nature and concentration. Perchlorate salts of the various cations were used. In all measurements, the ionic strength of the solution was kept constant at 0.1 M by addition of TBA⁺PF₆⁻ as an inert electrolyte. (A) Dependence upon Li⁺ concentration of the ζ -potential of undyed TiO₂ (b) and Ru(II)(dcbpy)₂(NCS)₂-derivatized oxide particles (d). Points labeled “a” (\blacktriangle) and “c” (\blacklozenge) represent ζ -potentials of naked and dyed particles, respectively, in solutions containing only (TBA⁺)PF₆⁻ ($[Li^+] = 0$). (B) Dependence upon Mg²⁺, Li⁺, Na⁺, and K⁺ cations concentration of the ζ -potential of undyed titanium dioxide colloidal particles.

than 150 ppm. The influence of water, deliberately added to the sample, was also tested. Addition of up to 1000 ppm of water did not affect the kinetics measured in the presence of LiI 0.1 M. In the case of TBAI 0.1 M, a fast initial kinetic phase was observed in the first 400 ns (Figure 2, trace b), which disappeared gradually when water was added. In these conditions, the value of $1/t_{1/2}$ diminished from 5×10^6 to 2×10^5 s⁻¹ when water content was increased from 50 to 1000 ppm. The long time feature of the reaction observed in the micro-seconds frame, however, was not affected by addition of water. This distinct behavior allows to conclude that the effects observed upon addition of various salts is not due to water added inadvertently.

Electrophoretic measurements were carried out to correlate the observed kinetic effects of the addition of small cations to a change of the particles surface charge. The latter is indeed expected to be primarily controlled by specific adsorption of ionic species in the inner Helmholtz layer at the interface. In Figure 4 A, the point labeled “a” represents the ζ -potential of TiO₂ colloidal particles recorded in the presence of (TBA⁺)(PF₆⁻). These bulky ions do not adsorb specifically on the oxide surface. The value of $\zeta = -17$ mV measured in this electrolyte is therefore representative of the surface charge of blank TiO₂

particles. This negative charge is probably due to Cl^- impurities originating from the TiCl_4 precursor used in the preparation of TiO_2 . When lithium ions are added to the electrolyte (curve b), the potential gradually increases with increasing Li^+ concentration and reverses from negative to positive at $[\text{Li}^+] = 3 \times 10^{-4}$ M.

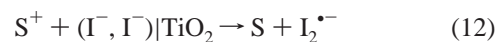
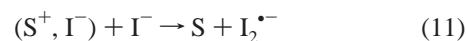
A similar experiment was carried out with dyed particles. The heat-treated TiO_2 powder was soaked in a solution of the Ru(II) dye in absolute ethanol, carefully washed, filtered, and dried, before being redispersed in propylene carbonate. The sensitizer used in this study was a dianion species, whose counterions were TBA^+ . As a result of the adsorption of the negatively charged dye sensitizer on the oxide surface, the ζ -potential was shifted negatively by approximately 10 mV (point labeled "c" in Figure 4A). Recent studies suggest that during adsorption of the dianion of the sensitizer one TBA^+ counterion penetrates the Stern layer and contributes to lower electrostatic repulsion between dye molecules. The second TBA^+ counterion remaining outside of the layer, the net overall charge per adsorbed dye molecule would thus be -1 .¹³ Under these conditions, a larger quantity of Li^+ is required to balance the negative charge, and the point of zero ζ -potential (PZZP) is consequently shifted by 1 order of magnitude to a higher concentration $[\text{Li}^+] = 3 \times 10^{-3}$ M.

Figure 4B shows the results obtained with other potential-determining cations. Among them, Mg^{2+} is clearly the most efficient one. The addition of a concentration as low as 2×10^{-4} M of magnesium dication was able to increase the ζ -potential of the oxide colloid from -17 to $+45$ mV. The PZZP established in this case at 3×10^{-5} M, which is 10 times lower than that obtained in the presence of Li^+ , and approximately 2 orders of magnitude lower than that measured with Na^+ and K^+ cations. Logically, values obtained for PZZP were found to correlate with the charge density δ of the cations, which follows the sequence Mg^{2+} ($\delta = 1.7 \text{ e}\text{\AA}^{-3}$) > Li^+ ($\delta = 1.1 \text{ e}\text{\AA}^{-3}$) > Na^+ ($\delta = 0.2 \text{ e}\text{\AA}^{-3}$) > K^+ ($\delta = 0.1 \text{ e}\text{\AA}^{-3}$).¹⁴

Adsorption of iodide anions onto the TiO_2 surface was monitored by using the same electrophoretic method. Provided that the particles were initially positively charged by adsorption of cations, substituting bulky counterions, such as ClO_4^- and PF_6^- , gradually by iodide yielded a continuous drop of the ζ -potential until the surface charge of the particles was partially neutralized. In the presence of Mg^{2+} 5×10^{-3} M, addition of 10^{-1} M I^- caused the surface potential to decrease from $+45$ mV to less than $+5$ mV. This potential drop upon addition of iodide was observed for undyed particles as well as for sensitized colloids, thus indicating that I^- ions are indeed able to adsorb within the Helmholtz layer of positively charged particles, despite the presence of bulky dye molecules covering the surface.

The step observed in the reaction kinetics when the lithium ions concentration is increased suggests that there might be at least two different mechanisms for the iodide oxidation reaction that prevail in different conditions. The slower kinetic path, which corresponds most probably to the thermodynamically unfavorable oxidation of I^- to iodine atom, should be preponderantly followed in the absence or at low concentrations of an active cation species.

Because a concentration of iodide of 10^{-1} M implies that ions are separated on the average by more than 25 \AA in the solution, simultaneous encounter of S^+ with two I^- species is fairly improbable. Reaction 8, which is the more energetically favorable route for iodide oxidation, should therefore imply prior formation of (S^+, I^-) and/or (I^-, I^-) ion pairs (eqs 11 and 12):



The formation of a complex between the oxidized state of a Ru(II) complex and the redox mediator has already been suggested.^{6a} Interaction between I^- and the sulfur atom of the thiocyanate ligands in our sensitizer can play in this respect a significant role. Ion pairing in this case would not require the semiconductor particles to be positively charged, because the $-\text{NCS}$ groups are at the frontier of the Stern layer and interaction with a free diffusing iodide is possible. Electrophoretic experiments showed however that the observed transition to a faster kinetic path is apparently a consequence of the reversal of the particle surface charge upon adsorption of potential-determining species, which causes I^- to efficiently adsorb onto the oxide. These observations strongly suggest that adsorption of potential-determining cations onto TiO_2 nanoparticles governs the formation of (I^-, I^-) ion pairs on the surface and allows the more energetically favorable and faster mechanism involving oxidation of I^- to $\text{I}_2^{\bullet-}$ to take place.

Conclusion

The kinetics of the oxidation of iodide by the oxidized state of *cis*-Ru^{II}(dcbpy)₂(NCS)₂ sensitizer adsorbed on nanocrystalline TiO_2 films was measured by transient laser spectroscopy. The rate of the reaction leading to the regeneration of the dye ground state was found to depend strongly on the nature and concentration of cations present in the solution. A brusque acceleration of the electron transfer process was observed at a critical concentration. Electrophoretic measurements show that this concentration corresponds to the reversal of the titanium dioxide particle surface charge from negative to positive upon adsorption of potential determining species. This observation is interpreted in terms of a transition between two reaction mechanisms characterized by different rate constants. The slower reaction path, that does not require the iodide anions to be adsorbed onto the surface, is attributed to the thermodynamically unfavorable oxidation of I^- to iodine radical atom. Alternatively, the encounter of a (S^+, I^-) complex with a second iodide ion could yield $\text{I}_2^{\bullet-}$ as a product of the electron transfer process. These mechanisms should be prevalent as long as the solid surface is negatively charged. When the surface charge is reversed to positive upon adsorption of cations, a faster reaction mechanism becomes predominant. Because it requires the adsorption of I^- on TiO_2 , the latter is identified as being due to the thermodynamically more favorable oxidation of I^- to $\text{I}_2^{\bullet-}$ that involves prior formation of (I^-, I^-) ions pairs on the surface.

Acknowledgment. Financial support of this work by the Swiss National Science Foundation (FNRS) is gratefully acknowledged.

References and Notes

- (1) (a) Rehm, J. M.; McLendon, G. L.; Nagasawa, Y.; Yoshihara, K.; Moser, J.; Grätzel, M. *J. Phys. Chem.* **1996**, *100*, 2820. (b) Burfeindt, B.; Hannappel, T.; Storck, W.; Willig, F. *J. Phys. Chem.* **1996**, *100*, 16463. (c) Tachibana, Y.; Moser, J. E.; Grätzel, M.; Klug, D. R.; Durrant, J. R. *J. Phys. Chem.* **1996**, *100*, 20056. (d) Asbury, J. B.; Ellingson, R. J.; Ghosh, H. N.; Ferrere, S.; Nozik, A. J.; Lian, T. *J. Phys. Chem. B* **1999**, *103*, 3110. (e) Hilgendorff, M.; Sundström, V. *J. Phys. Chem. B* **1998**, *102*, 10505. (f) Wachtveitl, J.; Huber, R.; Spörlein, S.; Moser, J. E.; Grätzel, M. *Int. J. Photoenergy* **1999**, *1*, 131.

- (2) (a) Moser, J. E.; Grätzel, M. *Chimia* **1998**, *52*, 160. (b) Moser, J. E.; Wolf, M.; Lenzmann, F.; Grätzel, M. *Z. Phys. Chem.* **1999**, *212*, 85.
- (3) (a) Moser, J. E.; Grätzel, M. *Chem. Phys.* **1993**, *176*, 493. (b) Moser, J. E. *Sol. Energy Mater. Sol. Cells* **1995**, *38*, 343. (c) Haque, S. A.; Tachibana, Y.; Klug, D. R.; Durrant, J. R. *J. Phys. Chem. B* **1998**, *102*, 1745.
- (4) (a) O'Regan, B.; Moser, J.; Anderson, M.; Grätzel, M. *J. Phys. Chem.* **1990**, *94*, 8720. (b) Nazeeruddin, M. K.; Liska, P.; Moser, J.; Vlachopoulos, N.; Grätzel, M. *Helv. Chim. Acta* **1990**, *73*, 1788.
- (5) (a) O'Regan, B.; Grätzel, M. *Nature* **1991**, *353*, 737. (b) Nazeeruddin, M. K.; Kay, A.; Rodicio, I.; Humphry-Baker, R.; Müller, E.; Liska, P.; Vlachopoulos, N.; Grätzel, M. *J. Am. Chem. Soc.* **1993**, *115*, 6382.
- (6) (a) Fitzmaurice, D. I.; Frei, H. *Langmuir* **1991**, *7*, 1129. (b) Myung, N.; Licht, S. *J. Electrochem. Soc.* **1995**, *142*, L129. (c) Nasr, C.; Hotchandani, S.; Kamat, P. V. *J. Phys. Chem. B* **1998**, *102*, 4944.
- (7) (a) Nord, G. *Comments Inorg. Chem.* **1992**, *13*, 221. (b) Alebbi, M.; Bignozzi, C. A.; Heimer, T. A.; Hasselmann, G. M.; Meyer, G. J. *J. Phys. Chem. B* **1998**, *102*, 7577.
- (8) Moser, J.; Grätzel, M. *Helv. Chim. Acta* **1982**, *65*, 1436.
- (9) (a) Kelly, C. A.; Farzad, F.; Thompson, D. W.; Stipkala, J. M.; Meyer, G. J. *Langmuir* **1999**, *15*, 7047. (b) Tachibana, Y.; Haque, S. A.; Willis, R. L.; Mercer, I. P.; Moser, J. E.; Klug, D. R.; Durrant, J. R. *J. Phys. Chem. B*, submitted.
- (10) Barbé, C. J.; Arendse, F.; Comte, P.; Jirousek, M.; Lenzmann, F.; Shklover, V.; Grätzel, M. *J. Am. Ceram. Soc.* **1997**, *80*, 3157.
- (11) Moser, J. E.; Noukakis, D.; Bach, U.; Tachibana, Y.; Klug, D. R.; Durrant, J. R.; Humphry-Baker, R.; Grätzel, M. *J. Phys. Chem. B* **1998**, *102*, 3649.
- (12) Hunter, R. J. *Introduction to Modern Colloid Science*; Oxford University Press: Oxford, 1993; Chapters 7 and 8.
- (13) Nazeeruddin, M. K.; Zakeeruddin, S. M.; Humphry-Baker, R.; Jirousek, M.; Liska, P.; Vlachopoulos, N.; Shklover, V.; Fischer, C. H.; Grätzel, M. *Inorg. Chem.* **1999**, *38*, 6298.
- (14) Charge densities of the cations were calculated using the ionic radii (Li⁺, 0.60 Å; Mg²⁺, 0.65 Å; Na⁺, 1.02 Å; K⁺, 1.38 Å) reported in the following: Shannon, R. D.; Prewitt, C. T. *Acta Crystallogr.* **1969**, *B25*, 925.